Supplement of Clim. Past, 14, 1179–1194, 2018
https://doi.org/10.5194/cp-14-1179-2018-supplement

Climate of the Past
Open Access
EGU

Supplement of

Solar and volcanic forcing of North Atlantic climate inferred from a process-based reconstruction

Jesper Sjolte et al.

Correspondence to: Jesper Sjolte (jesper.sjolte@geol.lu.se)

Table S1. Tropical eruptions during 1241-1970 CE of larger or similar magnitude as the 1991 Pinatubo eruption ($\sim$ -6 Wm^{-2}). All data from Sigl et al. (2015). UE indicates unknown source of eruption.

Name	Year	Estimated magnitude [Wm^{-2}]
UE 1836	1836	-6.57
UE 1832	1832	-6.46
Tambora/Indonesia	1815	-17.20
UE 1809	1809	-12.01
UE 1695	1695	-10.24
Parker/Philippines	1641	-11.84
Huaynaputina/Peru	1601	-11.58
Kuwae/Vanuatu	1458	-20.55
El Chichon?/Mexico	1345	-9.40
Quilotoa?/Ecuador	1286	-9.69
UE 1276	1276	-7.71
Samalas/Indonisia	1258	-32.79

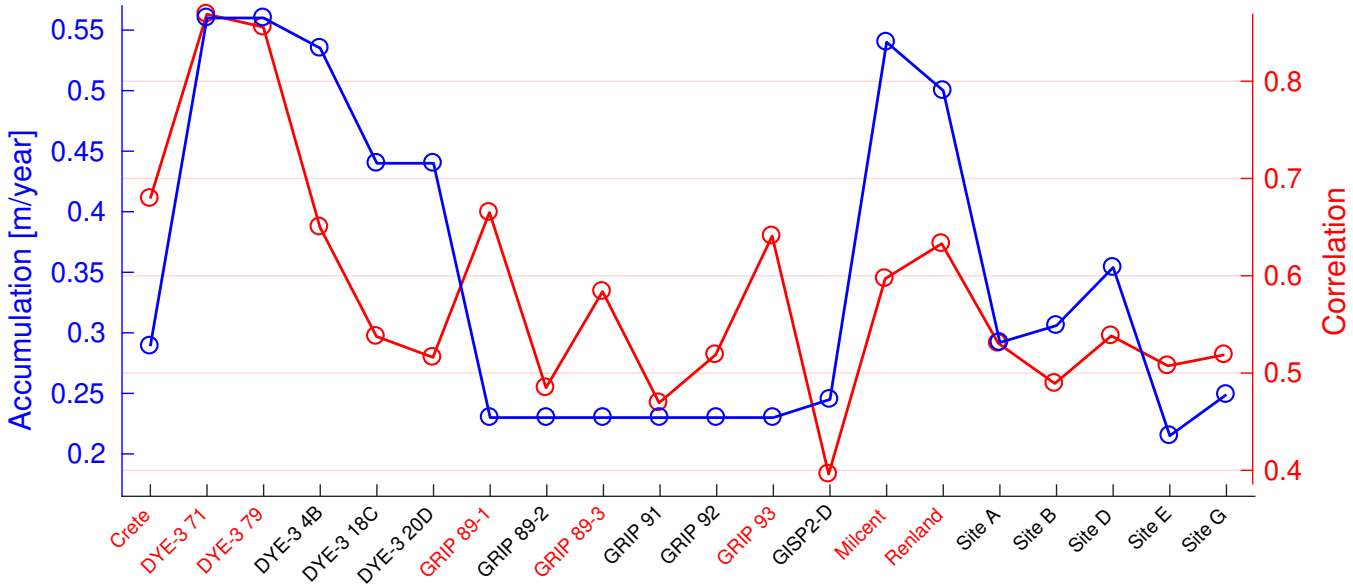

Figure S1. Accumulation at ice core sites (blue) and correlation between reconstructed winter δ^{18}O and ice core winter δ^{18}O (Vinther et al., 2010) 1778-1970 (red). The names of the ice core sites used in the reconstruction are written in red.

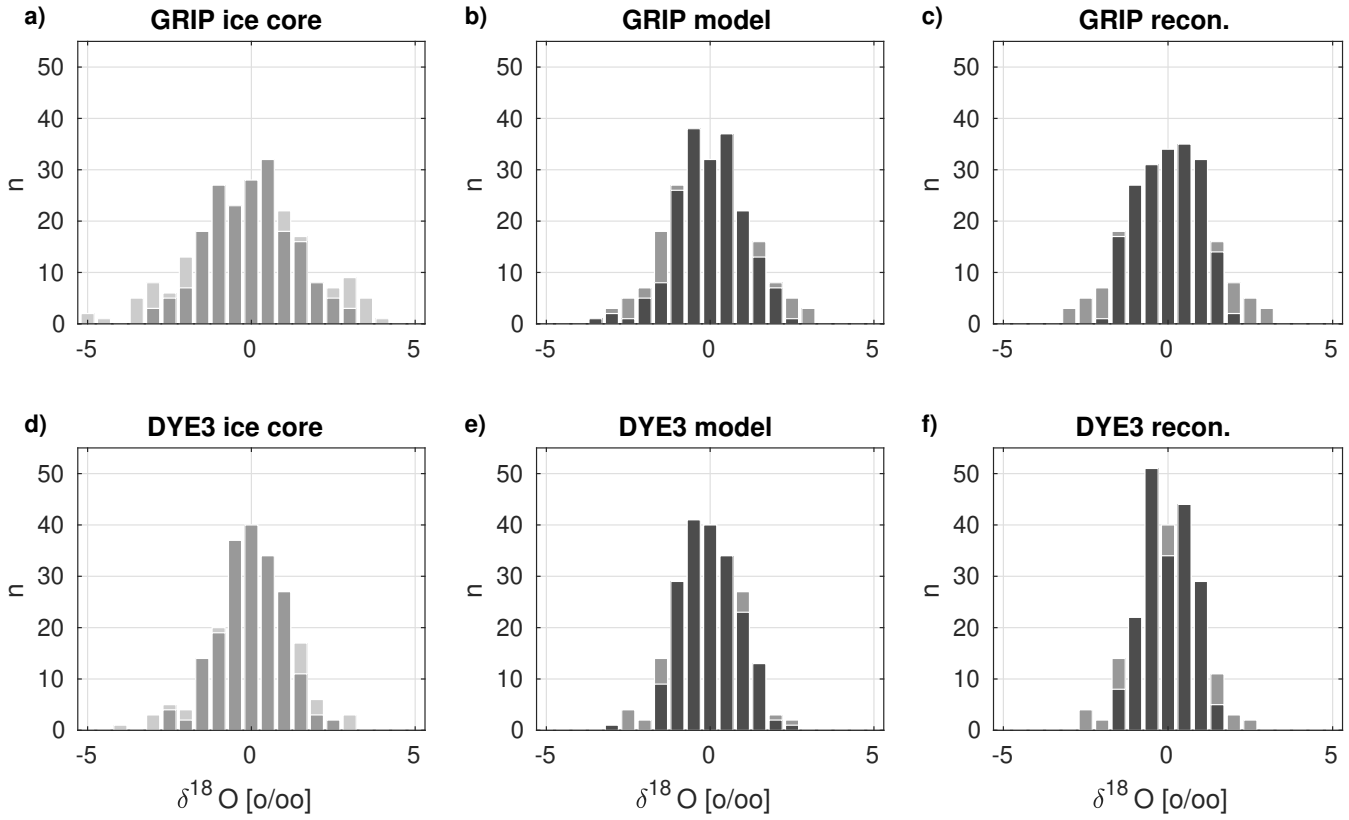

Figure S2. Histograms of ice core δ^{18}O and modeled δ^{18}O for winter covering the period 1778-1970. **a** Histogram of stacked GRIP δ^{18}O (6 cores, gray), with δ^{18}O for a single core plotted in the background in light gray to illustrate reduction of variability from stacking. **b** modeled GRIP δ^{18}O (dark gray) with stacked ice core δ^{18}O plotted in the background for comparison. **c** same as **b**, but for reconstructed δ^{18}O. **d, e, f**, same as **a, b, c**, but for DYE3. This figure both illustrates the inherent noise in ice core data, which can be reduced by using multiple cores, and shows that the model reconstruction covers most of the range of the ice core variability. Stacking even more ice core records (if available) could possible reduce the variability further. DYE3 has about twice the annual accumulation rate of GRIP, which also reduces the scatter

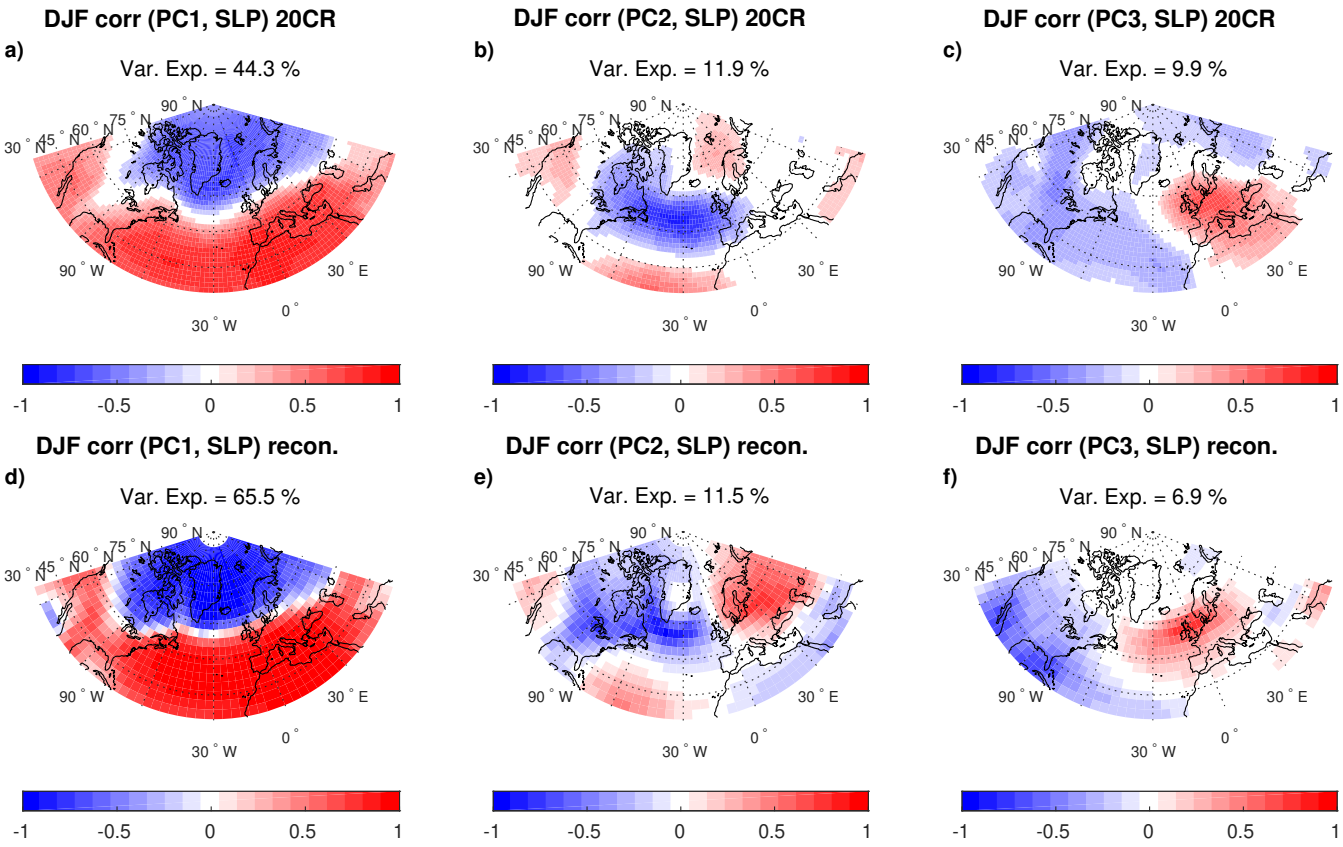

Figure S3. a Grid point correlation between 20CR SLP PC1 and 20CR SLP, **b** grid point correlation between 20CR SLP PC2 and 20CR SLP, and **c** grid point correlation between 20CR SLP PC3 and 20CR SLP. **d, e, f** same as **a, b, c** but for reconstructed PC1, PC2, PC3 and SLP. The explained variability of the PCs is indicated by each subplot. Only significant values of correlation are plotted ($p < 0.05$).

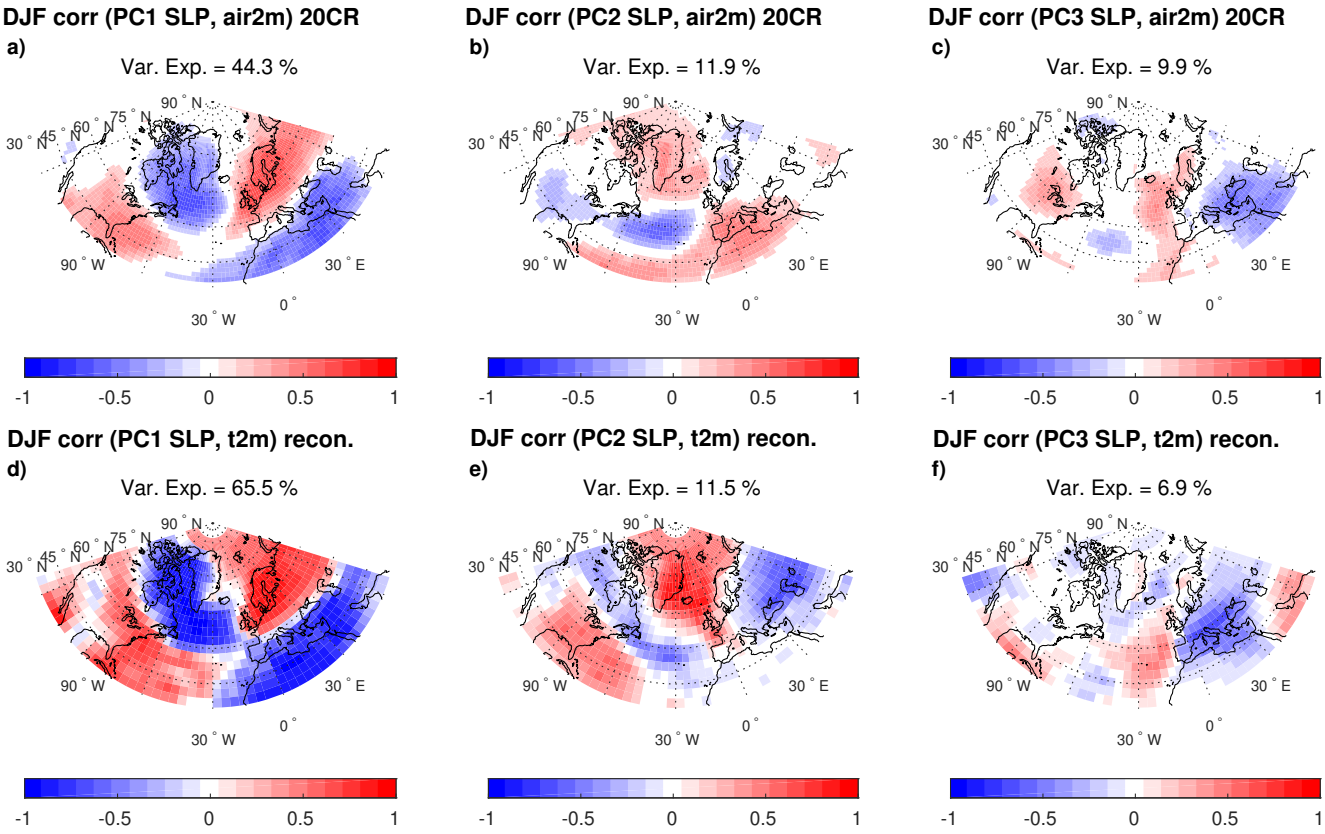

Figure S4. Same as Figure S3 but for correlation between PC1 (**a, d**), PC2 (**b, e**) and PC3 (**c, f**) of SLP and T2m. Only significant values of correlation are plotted ($p < 0.05$).

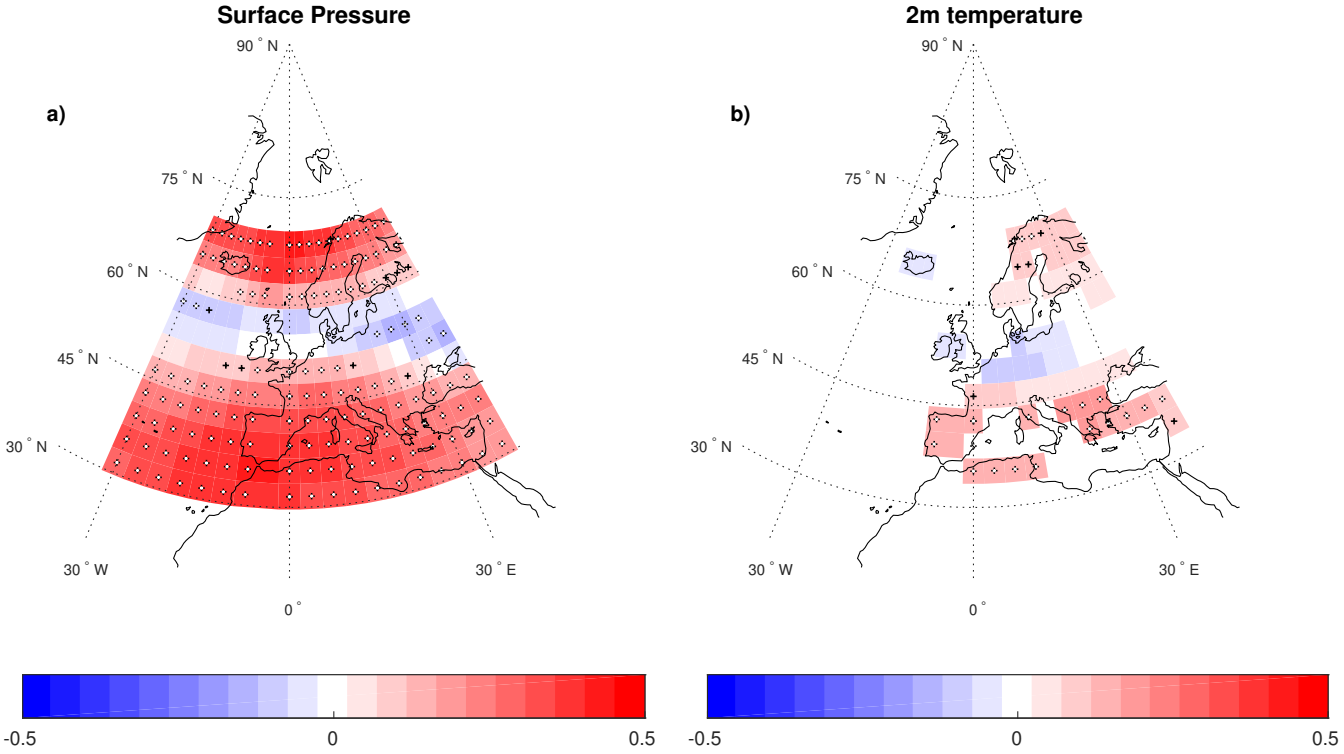

Figure S5. a Grid point correlation between reconstructed SLP (this study) and reconstructed SLP by Luterbacher et al. (2001). **b** Same as **a**, but for T2m (Luterbacher et al., 2004). The data covers the period (1659-1970) with the data by interpolated Luterbacher et al. to the model grid of our reconstruction (lat. x lon. $\sim 3.75^o$ x 3.75^o). The black stippling indicates significance of $p < 0.1$ and the white indicates $p < 0.05$.

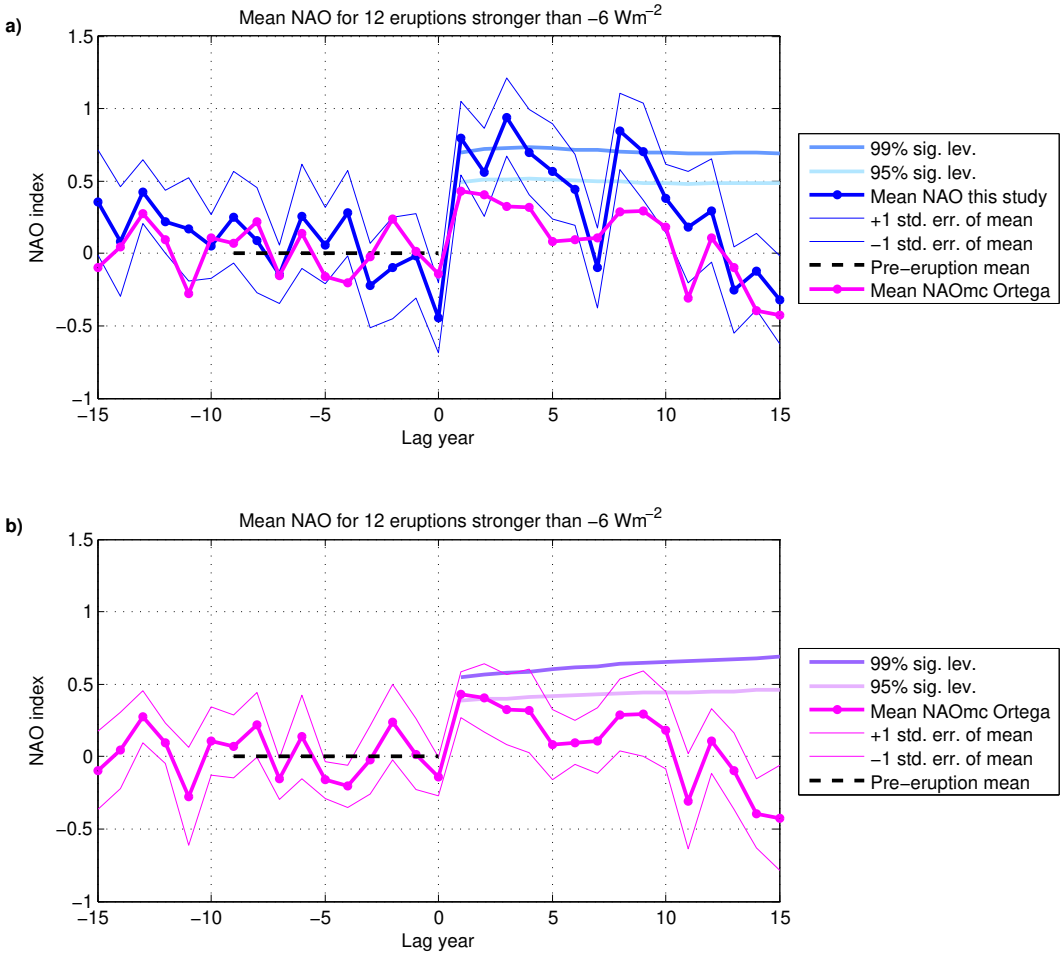

Figure S6. Superimposed epoch analysis of the mean response in NAO to the 12 largest tropical volcanic eruptions (Sigl et al., 2015) (Table S3). **a** Mean response in reconstructed NAO (blue) with the time series normalized to the mean NAO of the 10 years preceding the eruption. For comparison the same analysis is carried out for the NAOmc reconstruction (magenta) by Ortega et al. (2015). The significance levels in **a** are estimated from 100,000 random samples of 12 years drawn from the reconstructed NAO. **b** Same analysis as in **a**. but carried out for the NAOmc reconstruction (magenta) by Ortega et al. (2015) including significance levels. Note the sloping significance levels in figure **b** compared to figure **a** due to larger auto-correlation of the reconstruction by Ortega et al. (2015).

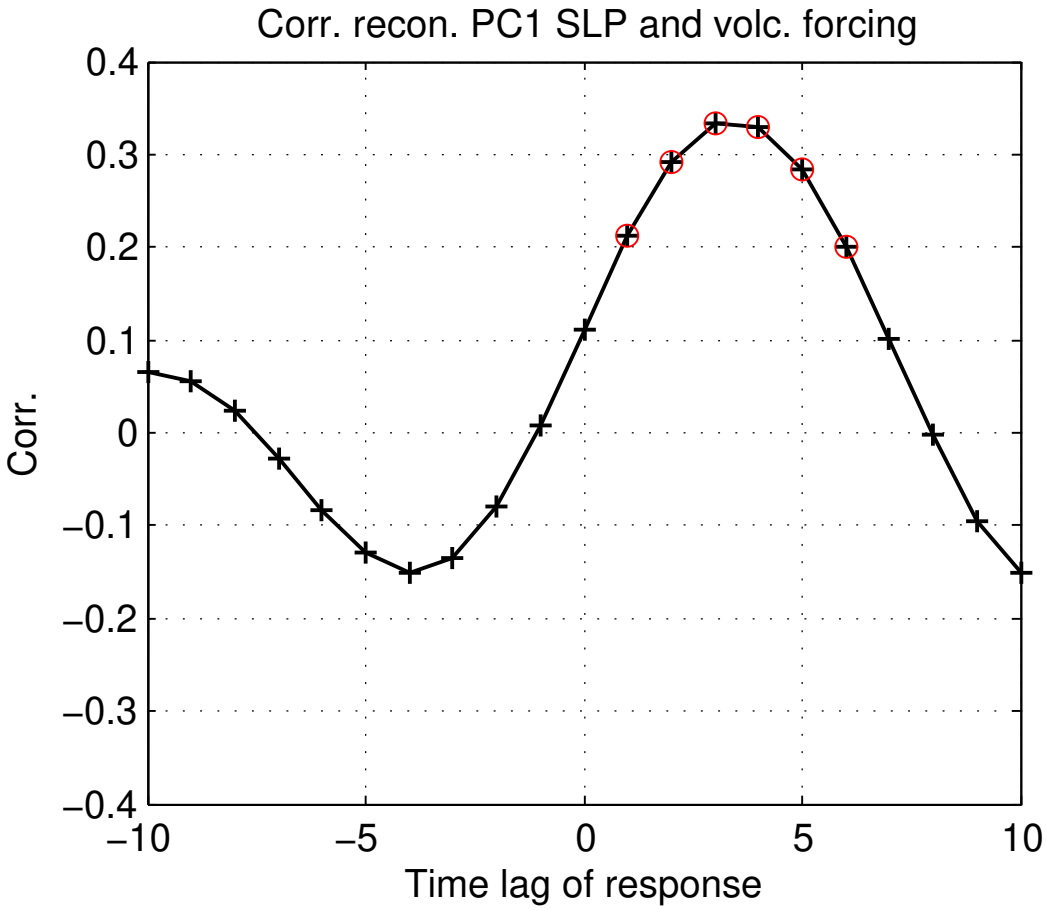

Figure S7. Time lag correlation analysis between reconstructed NAO and tropical volcanic eruptions (30^{o}N-30^{o}S) (Toohey and Sigl, 2017). Both data series are band-pass filtered (1/10 to 1/100 cycles per year). The red circles indicate significant correlation ($p < 0.01$) calculated with the random-phase test by Ebisuzaki (1997) to take into account auto-correlation.

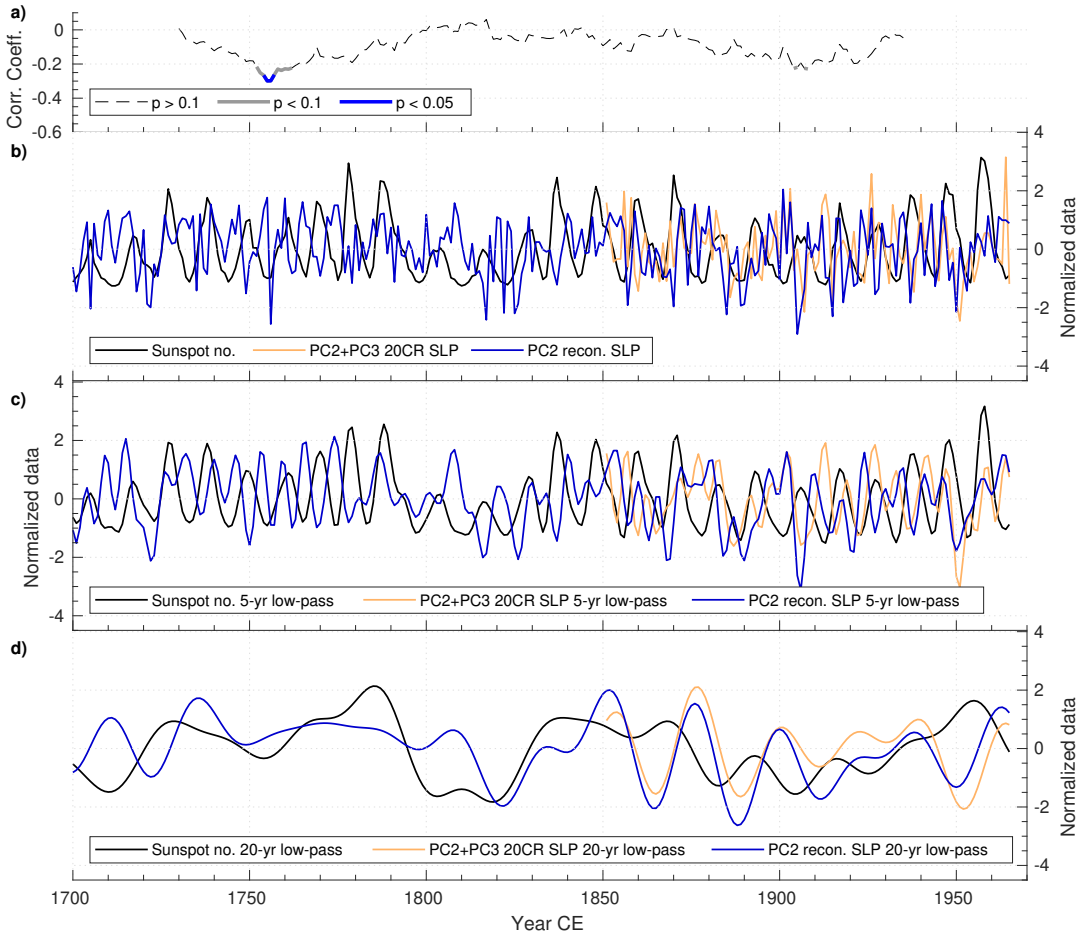

Figure S8. Reconstructed PC2 of SLP plotted with the sunspot number. **a** Moving 61-point correlation between reconstructed PC2 of SLP and the sunspot number. **b** Time series of the sunspot number, PC2+PC3 of 20CR SLP (see text and Table 4) and PC2 of reconstructed SLP. **c** Same as **b**, except filtered with a 5-year low-pass filter. **d** Same as **b**, except filtered with a 20-year low-pass filter.

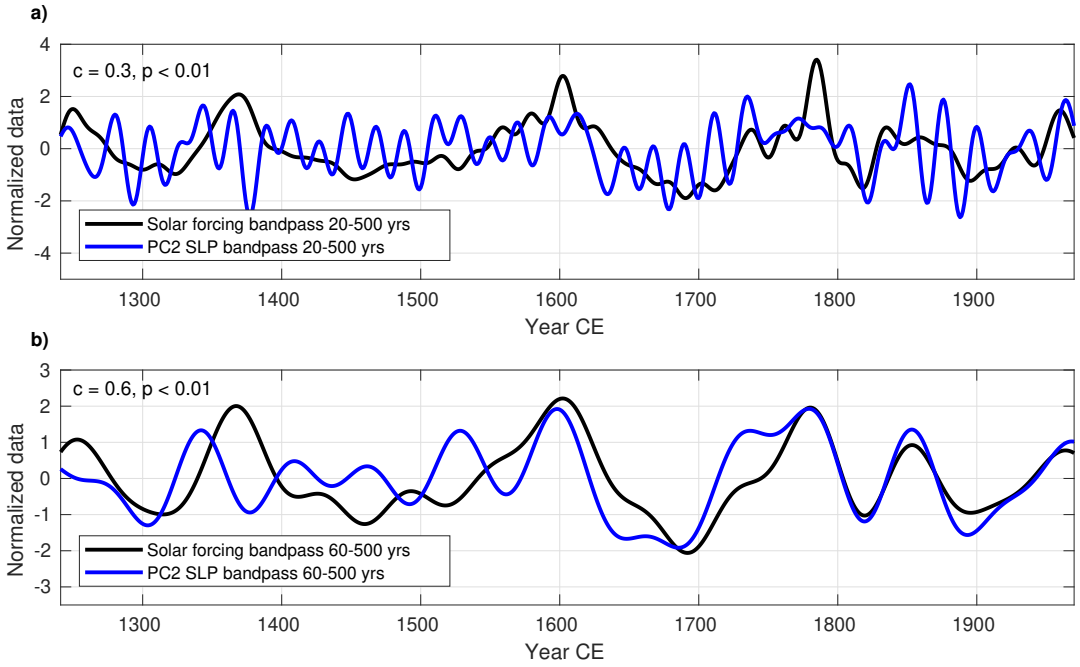

Figure S9. PC2 of reconstructed SLP plotted with reconstructed solar forcing (Muscheler et al., 2016) using a band-pass filter for **a** 20-500 year periodicities, and **b** 60-500 year periodicities. All correlations are for detrended data and p-values calculated with the random-phase test by Ebisuzaki (1997) to take into account auto-correlation.

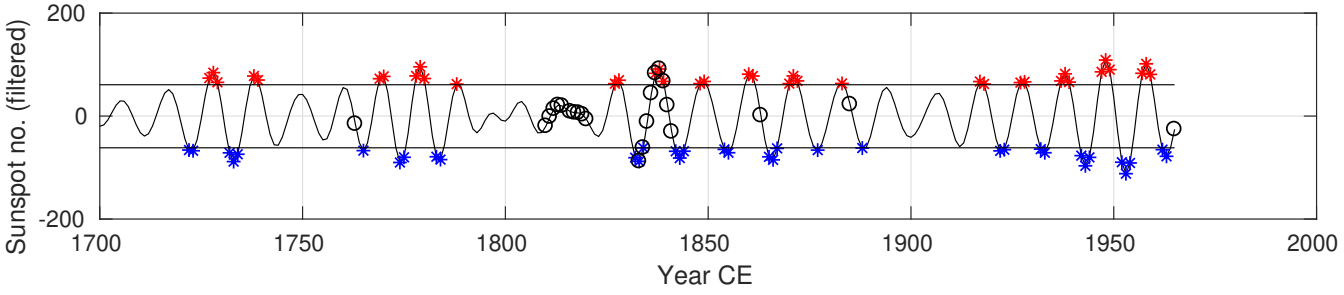

Figure S10. Band-pass filtered (8-13 year periodicity) sunspot number (Clette and Lefèvre, 2016) and years selected for solar maximum (red) and solar minimum (blue). We pick a maximum of three years around each maximum and minimum, and furthermore employ a threshold of 1.25 standard deviations. The horizontal lines mark $\pm$ 1.25 standard deviations. The motivation for the threshold of 1.25 standard deviation is to obtain the most extreme values of solar maximum and minimum, while still selecting enough years to get good sampling statistics. We removed 5 years following major tropical volcanic eruptions ($<$ -6 Wm^{-2}) and 1 year following minor tropical volcanic eruptions ($>$ -6 Wm^{-2}) from the analysis. These years are marked with black circles.

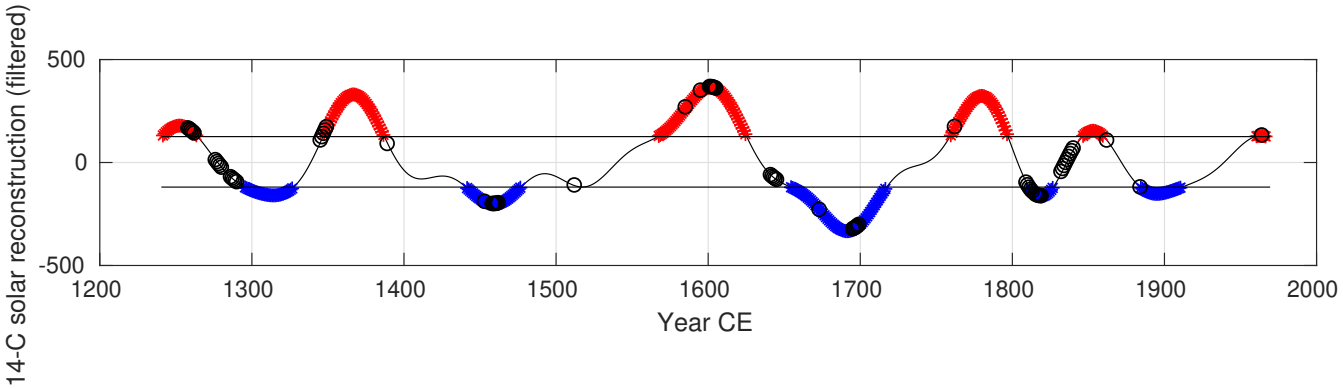

Figure S11. Band-pass filtered (60-500 year periodicity) ^{14}C data (Muscheler et al., 2016) and years selected for solar maximum (red) and solar minimum (blue). The horizontal lines mark $\pm$ 0.75 standard deviations. The motivation for the threshold of 0.75 standard deviation is to obtain the most extreme values of solar maximum and minimum, while still selecting enough years to get good sampling statistics. We removed 5 years following major tropical volcanic eruptions ($<$ -6 Wm^{-2}) and 1 year following minor tropical volcanic eruptions ($>$ -6 Wm^{-2}) from the analysis. These years are marked with black circles.

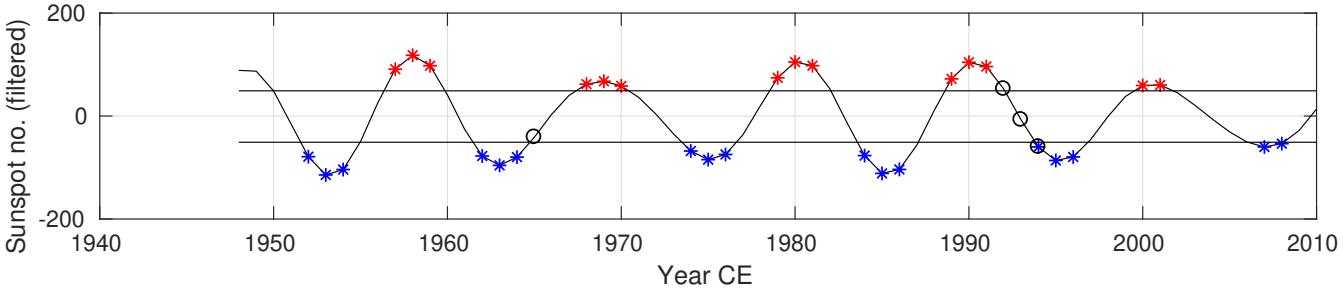

Figure S12. Band-pass filtered (8-13 year periodicity) sunspot number (Clette and Lefèvre, 2016) and years selected for solar maximum (red) and solar minimum (blue) for Figure 5 (20CR (1948-2010) atmospheric response to solar forcing). We pick a maximum of three years around each maximum and minimum, and furthermore employ a threshold of 0.75 standard deviations. The horizontal lines mark $\pm$ 0.75 standard deviations. The motivation for the threshold of 0.75 standard deviations is to obtain the most extreme values of solar maximum and minimum, while still selecting enough years to get good sampling statistics. We removed the 3 years following the Pinatubo eruption in 1991 and 1 year following the Agung eruption in 1964. These years are marked with black circles.

References

Clette, F. and Lefèvre, L.: The New Sunspot Number: Assembling All Corrections, Solar Physics, 291, 2629–2651, https://doi.org/10.1007/s11207-016-1014-y, https://doi.org/10.1007/s11207-016-1014-y, 2016.

Ebisuzaki, W.: A method to estimate the statistical significance of a correlation when the data are serially correlated, JOURNAL OF CLIMATE, 10, 2147–2153, https://doi.org/10.1175/1520-0442(1997)010<2147:AMTETS>2.0.CO;2, 1997.

Luterbacher, J., Xoplaki, E., Dietrich, D., Jones, P. D., Davies, T. D., Portis, D., Gonzalez-Rouco, J. F., von Storch, H., Gyalistras, D., Casty, C., and Wanner, H.: Extending North Atlantic oscillation reconstructions back to 1500, Atmospheric Science Letters, 2, 114–124, https://doi.org/10.1006/asle.2002.0047, http://dx.doi.org/10.1006/asle.2002.0047, 2001.

Luterbacher, J., Dietrich, D., Xoplaki, E., Grosjean, M., and Wanner, H.: European seasonal and annual temperature variability, trends, and extremes since 1500, SCIENCE, 303, 1499–1503, https://doi.org/10.1126/science.1093877, 2004.

Muscheler, R., Adolphi, F., Herbst, K., and Nilsson, A.: The Revised Sunspot Record in Comparison to Cosmogenic Radionuclide-Based Solar Activity Reconstructions, Solar Physics, 291, 3025–3043, https://doi.org/10.1007/s11207-016-0969-z, http://dx.doi.org/10.1007/s11207-016-0969-z, 2016.

Ortega, P., Lehner, F., Swingedouw, D., Masson-Delmotte, V., Raible, C. C., Casado, M., and Yiou, P.: A model-tested North Atlantic Oscillation reconstruction for the past millennium, NATURE, 523, 71+, https://doi.org/10.1038/nature14518, 2015.

Sigl, M., Winstrup, M., McConnell, J. R., Welten, K. C., Plunkett, G., Ludlow, F., Buentgen, U., Caffee, M., Chellman, N., Dahl-Jensen, D., Fischer, H., Kipfstuhl, S., Kostick, C., Maselli, O. J., Mekhaldi, F., Mulvaney, R., Muscheler, R., Pasteris, D. R., Pilcher, J. R., Salzer, M., Schuepbach, S., Steffensen, J. P., Vinther, B. M., and Woodruff, T. E.: Timing and climate forcing of volcanic eruptions for the past 2,500 years, NATURE, 523, 543+, https://doi.org/10.1038/nature14565, 2015.

Toohey, M. and Sigl, M.: Volcanic stratospheric sulfur injections and aerosol optical depth from 500 BCE to 1900 CE, Earth System Science Data, 9, 809–831, https://doi.org/10.5194/essd-9-809-2017, https://www.earth-syst-sci-data.net/9/809/2017/, 2017.

Vinther, B., Jones, P., Briffa, K., Clausen, H., Andersen, K., Dahl-Jensen, D., and Johnsen, S.: Climatic signals in multiple highly resolved stable isotope records from Greenland, Quaternary Science Reviews, 29, 522 – 538, https://doi.org/http://dx.doi.org/10.1016/j.quascirev.2009.11.002, http://www.sciencedirect.com/science/article/pii/S0277379109003655, 2010.